

A Unified Approach to the Design of Adaptive and Repetitive Controllers for Robotic Manipulators

Nader Sadegh

Assistant Professor,
The George W. Woodruff School of
Mechanical Engineering,
Georgia Institute of Technology,
Atlanta, GA 30332

Roberto Horowitz

Associate Professor.

Wei-Wen Kao

Graduate Student.

Masayoshi Tomizuka

Professor.

Department of Mechanical Engineering,
University of California at Berkeley,
Berkeley, CA 94720

A unified approach, based on Lyapunov theory, for synthesis and stability analysis of adaptive and repetitive controllers for mechanical manipulators is presented. This approach utilizes the passivity properties of the manipulator dynamics to derive control laws which guarantee asymptotic trajectory following, without requiring exact knowledge of the manipulator dynamic parameters. The manipulator overall controller consists of a fixed PD action and an adaptive and/or repetitive action for feed-forward compensations. The nonlinear feedforward compensation is adjusted utilizing a linear combination of the tracking velocity and position errors. The repetitive compensator is recommended for tasks in which the desired trajectory is periodic. The repetitive control input is adjusted periodically without requiring knowledge of the explicit structure of the manipulator model. The adaptive compensator, on the other hand, may be used for more general trajectories. However, explicit information regarding the dynamic model structure is required in the parameter adaptation. For discrete time implementations, a hybrid version of the repetitive controller is derived and its global stability is proven. A simulation study is conducted to evaluate the performance of the repetitive controller, and its hybrid version. The hybrid repetitive controller is also implemented in the Berkeley/NSK SCARA type robot arm.

1 Introduction

In recent years there has been a substantial amount of research effort directed toward the development of adaptive control algorithms for robotic manipulators. What has made this problem so challenging to the robotic and control communities is the fact that most of the terms in the manipulator dynamic equations of motion are complicated nonlinear functions of the joint coordinates, and some are in addition quadratic functions of the joint velocities. However, most of the early works in the field, and even some recent works, neglect the nonlinear dependence of the manipulator parameters on the joint coordinates in the stability analysis, or rely on local linearization techniques to prove the stability of the schemes. For examples of these early works, the reader is referred to Dubowsky and DesForges (1979); Horowitz and Tomizuka (1980); and Takegaki and Arimoto (1981).

Some of the more recent works in this field, such as Slotine and Li (1986) and Sadegh and Horowitz (1987a), have successfully proven the global stability of the adaptive control schemes taking into account the complete nonlinear model of

the manipulator dynamics. Two key observations regarding the structure of manipulator dynamics have made the global stability proofs possible. The first observation is based on the fact that the asymptotic convergence of most Parameter Adaptation Algorithms (PAA) can only be proven if the parameters being estimated remain constant. Thus, in order to estimate unknown inertial terms in the manipulator dynamic equations, nonlinear terms, which are functions of the joint coordinates, are reparametrized into a product of a matrix function of the joint coordinates, *which is assumed to be known*, and a *constant unknown vector*, which is dependent on the manipulator inertial parameters. For examples of the use of this technique, the reader is referred to the works by Khosla and Kanade (1985); Atketson et al. (1985); Craig et al. (1986); Slotine and Li (1986); and Sadegh and Horowitz (1987a). A major issue concerning the implementation of this technique is that the joint coordinate function matrix needs to be computed in real time. This may seriously limit the sampling rate of the control algorithm, since its computation involves a large number of transcendental functions of the joint coordinates.

The second observation is that, in spite of their nonlinear characteristics, mechanical manipulators are passive dynamical systems. The latter can be rigorously proven by utilizing the relationship between the generalized inertia matrix and the Coriolis and centripetal acceleration terms in the equations of

Contributed by the Dynamic Systems and Control Division for publication in the JOURNAL OF DYNAMIC SYSTEMS, MEASUREMENT, AND CONTROL. Manuscript received by the Dynamic Systems and Control Division May 23, 1988; revised manuscript received November 1989. Associate Editor: M. Donath.

motion. For examples, see Slotine and Li (1986) and Sadegh and Horowitz (1987a).

Parallel to the adaptive control effort, there has been a significant amount of research directed toward the development of so-called "learning," "betterment," or "repetitive" control schemes for robot manipulators. These schemes are utilized in applications where the robot is required to execute the same motion over and over again, with a certain periodicity. The basic idea behind these techniques is to improve the tracking performance from one cycle to the next by adjusting the input based on the error signals between the desired motion and the manipulator motion from the previous cycles. With consecutive iterations, the manipulator is expected to eventually "learn" the task, and execute the motion without any error. Works which utilize repetitive types of control algorithms include those of Arimoto et al. (1985), Atkeson and McIntyre (1986), Hara et al. (1985), and Tsai et al. (1988). Unfortunately, many of these works require some of the same assumptions concerning the linearization of manipulator dynamic equations as in early adaptive control works.

When a robot is expected to track a trajectory known in advance, such as in repetitive applications, the adaptive control schemes can be modified by incorporating a priori trajectory information to improve their performance. As presented in Sadegh and Horowitz (1987b), Bayard and Wen (1988), and Wen and Bayard (1988), the desired trajectory position, velocity, and acceleration signals can be used in the computation of the joint coordinate function matrix instead of the actual manipulator joint coordinates and velocities. As shown in Sadegh and Horowitz (1987b), an additional nonlinear term must be included in the control law to preserve the global asymptotic stability properties of the original scheme. The advantage of these modifications are two-fold. First, since the desired trajectories are known in advance, the computation of the joint coordinate matrix can be done off-line, resulting in considerable improvements in the computational efficiency of the control algorithm. Secondly, since the desired trajectory signals used in the PAA (Parameter Adaptation Algorithm) are not contaminated by noise, the PAA will yield unbiased estimates. Thus, the resulting adaptive system is more robust to stochastic input disturbances and sensor noises.

This paper extends the analysis techniques for adaptive control in Sadegh and Horowitz (1987b) to the synthesis and stability of repetitive control algorithms for robotic manipulators. The effectiveness of the repetitive control algorithms is demonstrated by simulation and experimental studies.

2 Dynamics of Robotic Manipulators

In this section we will review some important properties of the dynamic equations of motion for robotic manipulators comprised of serially connected rigid links. These properties will be utilized in the next section to derive nonadaptive, adaptive, and repetitive tracking control laws. Consider an n -link rigid manipulator expressed by

$$\frac{d}{dt}\dot{\mathbf{x}}_p(t) = \ddot{\mathbf{x}}_p(t) \quad (2.1)$$

$$\mathbf{M}(\mathbf{x}_p)\frac{d}{dt}\dot{\mathbf{x}}_p(t) = \mathbf{q}(t) - \mathbf{c}(\mathbf{x}_p, \dot{\mathbf{x}}_p) - \mathbf{g}(\mathbf{x}_p) - \mathbf{d}_m(\dot{\mathbf{x}}_p, \mathbf{q}) + \mathbf{d}_u$$

where \mathbf{x}_p is the $n \times 1$ vector of joint positions, $\dot{\mathbf{x}}_p$ is the $n \times 1$ vector of joint velocities, $\mathbf{M}(\mathbf{x}_p)$ is the $n \times n$ symmetric and positive definite matrix (also called the generalized inertia matrix), $\mathbf{q}(t)$ is the $n \times 1$ vector of joint torques of forces supplied by the actuators, $\mathbf{c}(\mathbf{x}_p, \dot{\mathbf{x}}_p)$ is the $n \times 1$ vector due to Coriolis and centripetal forces, $\mathbf{g}(\mathbf{x}_p)$ is the $n \times 1$ vector due to gravitational forces and $\mathbf{d}_m(\dot{\mathbf{x}}_p, \mathbf{q})$ is the $n \times 1$ vector due to friction forces. \mathbf{d}_u is the $n \times 1$ vector due to unmodelled disturbance forces.

$\mathbf{c}(\mathbf{x}_p, \dot{\mathbf{x}}_p)$ can be expressed in the following form

$$\mathbf{c}(\mathbf{x}_p, \dot{\mathbf{x}}_p) = \mathbf{C}(\mathbf{x}_p, \dot{\mathbf{x}}_p)\dot{\mathbf{x}}_p = \begin{bmatrix} \dot{\mathbf{x}}_p^T \mathbf{N}^1(\mathbf{x}_p) \dot{\mathbf{x}}_p \\ \dot{\mathbf{x}}_p^T \mathbf{N}^2(\mathbf{x}_p) \dot{\mathbf{x}}_p \\ \vdots \\ \dot{\mathbf{x}}_p^T \mathbf{N}^n(\mathbf{x}_p) \dot{\mathbf{x}}_p \end{bmatrix} \quad (2.2)$$

where the \mathbf{N}^i 's matrices are symmetric.

The following relation is satisfied between the \mathbf{N}^i 's matrices and the generalized inertia matrix \mathbf{M} (Sadegh, Horowitz (1987a))

$$\mathbf{N}^i(\mathbf{x}_p) = \frac{1}{2} \left[\frac{\partial \mathbf{m}_i}{\partial \mathbf{x}_p} + \left(\frac{\partial \mathbf{m}_i}{\partial \mathbf{x}_p} \right)^T - \frac{\partial \mathbf{M}}{\partial \mathbf{x}_{pi}} \right] \quad (2.3)$$

where \mathbf{m}_i is the i th row (or column) of \mathbf{M} and \mathbf{x}_{pi} is the i th element of \mathbf{x}_p .

The i th element of the friction force vector $\mathbf{d}_m(\dot{\mathbf{x}}_p, \mathbf{q})$ can be expressed as

$$d_{mi}(x_{vi}, q_i) = d_{ci}(x_{vi}, q_i) + d_{li}x_{vi}(t) \quad (2.4)$$

where $d_{ci}(x_{vi}, q_i)$ represents the Coulomb friction component and $d_{li}x_{vi}(t)$ represents the linear friction component. x_{vi} and q_i are the i th components of $\dot{\mathbf{x}}_p$ and \mathbf{q} , respectively.

Equation (2.1) can be rewritten in a more compact form by introducing the definition of the *covariant derivative*. Given a vector $\mathbf{v}_p(t) \in R^n$, the covariant derivative of $\mathbf{v}_p(t)$ along \mathbf{x}_p , denoted by $\frac{D}{dt}\mathbf{v}_p(t)$, is defined by

$$\frac{D}{dt}\mathbf{v}_p(t) = \frac{d}{dt}\mathbf{v}_p(t) + \mathbf{M}(\mathbf{x}_p)^{-1}\mathbf{C}(\mathbf{x}_p, \dot{\mathbf{x}}_p)\mathbf{v}_p, \quad (2.5)$$

where $\mathbf{M}(\mathbf{x}_p)$ is the generalized inertia matrix, and the i th element of the Coriolis vector $\mathbf{C}(\mathbf{x}_p, \dot{\mathbf{x}}_p)\mathbf{v}_p$, in equation (2.5) is given by

$$\mathbf{c}_i(\mathbf{x}_p, \dot{\mathbf{x}}_p)\mathbf{v}_p = \dot{\mathbf{x}}_p^T \mathbf{N}^i(\mathbf{x}_p)\mathbf{v}_p = \mathbf{v}_p^T \mathbf{N}^i(\mathbf{x}_p)\dot{\mathbf{x}}_p, \quad (2.6)$$

where $\mathbf{c}_i(\mathbf{x}_p, \dot{\mathbf{x}}_p)$ is the i th row of the matrix $\mathbf{C}(\mathbf{x}_p, \dot{\mathbf{x}}_p)$ in equation (2.2).

Utilizing the definitions in equations (2.5) and (2.6), equation (2.1) can be rewritten as

$$\mathbf{M}(\mathbf{x}_p)\frac{D}{dt}\dot{\mathbf{x}}_p(t) = \mathbf{f}_p(t), \quad (2.7)$$

$$\mathbf{f}_p = \mathbf{q}(t) - \mathbf{g}(\mathbf{x}_p) - \mathbf{d}_m(\dot{\mathbf{x}}_p, \mathbf{q}) + \mathbf{d}_u$$

Equation (2.7) is similar to the equation of motion of a single mass actuated by an external force, with the difference that the covariant derivative $\frac{D}{dt}$, is in place of the time derivative

$\frac{d}{dt}$. In fact, the covariant derivative has similar properties to those of the conventional time derivative. By using the definition of the covariant derivative, we can show that the following property holds: For any vectors \mathbf{v}_{1p} and \mathbf{v}_{2p} in R^n ,

$$\frac{d}{dt}\mathbf{v}_{1p}^T \mathbf{M}(\mathbf{x}_p)\mathbf{v}_{2p} = [\mathbf{M}(\mathbf{x}_p)\frac{D}{dt}\mathbf{v}_{1p}]^T \mathbf{v}_{2p} + \mathbf{v}_{1p}^T [\mathbf{M}(\mathbf{x}_p)\frac{D}{dt}\mathbf{v}_{2p}] \quad (2.8)$$

where $\mathbf{M}(\mathbf{x}_p)$ is the generalized inertia matrix. The formal proof of the property can be found in Sadegh (1987).

2.1 Reparametrization of the Manipulator Dynamic Equation. As was discussed by several authors (e.g., Khosla and Kanade (1985); Atkeson et al. (1985); and Craig et al. (1986)), the manipulator dynamic parameters $\mathbf{M}(\mathbf{x}_p)$, $\mathbf{C}(\mathbf{x}_p, \dot{\mathbf{x}}_p)$, and $\mathbf{g}(\mathbf{x}_p)$ can be reparametrized into products of *known* nonlinear functions of the joint coordinates and *constant* functions of the inertia properties of the manipulator and payload. Using this idea we define the $n \times m$ matrix $\mathbf{W}(\cdot)$ and the $m \times 1$ constant vector Θ such that, for any $n \times 1$ vectors \mathbf{v}_1 , \mathbf{v}_2 , \mathbf{v}_3 , and \mathbf{v}_4 , $\mathbf{W}(\cdot)$ and Θ are given by

$$\mathbf{W}(\mathbf{v}_1, \mathbf{v}_2, \mathbf{v}_3, \mathbf{v}_4)\boldsymbol{\Theta} = \mathbf{M}(\mathbf{v}_1)\mathbf{v}_4 + \mathbf{C}(\mathbf{v}_1, \mathbf{v}_2)\mathbf{v}_3 + \mathbf{g}(\mathbf{v}_1) \quad (2.9)$$

Notice that $\mathbf{W}(\mathbf{v}_1, \mathbf{v}_2, \mathbf{v}_3, \mathbf{v}_4)$ is a linear function of \mathbf{v}_4 and $\mathbf{W}(\mathbf{v}_1, \mathbf{v}_2, \mathbf{v}_3, \mathbf{v}_4) = \mathbf{W}(\mathbf{v}_1, \mathbf{v}_3, \mathbf{v}_2, \mathbf{v}_4)$.

Using equation (2.9), we can reparametrize the manipulator dynamic equation as follows:

$$\mathbf{M}(\mathbf{x}_p)\ddot{\mathbf{x}}_p + \mathbf{C}(\mathbf{x}_p, \dot{\mathbf{x}}_p)\dot{\mathbf{x}}_p + \mathbf{g}(\mathbf{x}_p) = \mathbf{W}(\mathbf{x}_p, \dot{\mathbf{x}}_p, \dot{\mathbf{x}}_p, \ddot{\mathbf{x}}_p)\boldsymbol{\Theta}. \quad (2.10)$$

3 Control of Robotic Manipulators Using the Desired Compensation Control Law (DCCL)

In this section we will discuss the motion control of robotic manipulators using a modification of the so called computed torque method. The control structure presented in this section will be utilized in subsequent sections in the design of both adaptive and repetitive controllers.

The control objective is to force the manipulator to track a set of given joint positions and velocities with desirable dynamics. We will denote the desired quantities by $\mathbf{x}_d(t)$ and $\dot{\mathbf{x}}_d(t)$ respectively. Assume that $\dot{\mathbf{x}}_d(t)$ is differentiable and denote its derivative by $\ddot{\mathbf{x}}_d(t)$, where $\ddot{\mathbf{x}}_d(t)$ is the vector of desired accelerations.

We first review the control scheme introduced in Slotine and Li (1986) and in Sadegh and Horowitz (1987a). This scheme employs an exact compensation for all the nonlinearities in the manipulator dynamics. Hence, we call this scheme the Exact Compensation Control Law (ECCL), also known in the robotics literature as the computed torque method. The control algorithm is a fixed PD controller plus a feed-forward inertia and Coriolis compensator. The control task is performed by employing an inner velocity and an outer position feedback loop. The inner velocity feedback loop contains the adaptation law and/or the repetitive law, if desired. The outer feedback loop is a fixed proportional position feedback.

Let $\mathbf{e}(t)$ denote the tracking position error vector:

$$\mathbf{e}(t) = \mathbf{x}_p(t) - \mathbf{x}_d(t) \quad (3.1)$$

In order to guarantee the asymptotic stability of the algorithm, we need to introduce an auxiliary signal, $\mathbf{v}_p(t)$, which is the reference velocity to the inner velocity loop (see Fig. 2). Its time derivative is denoted by $\mathbf{u}(t)$.

$$\mathbf{v}_p(t) = \dot{\mathbf{x}}_d(t) - \lambda_p \mathbf{e}(t) \quad \lambda_p > 0, \quad (3.2)$$

$$\mathbf{u}(t) = \frac{d}{dt} \mathbf{v}_p(t).$$

The reference velocity, $\mathbf{v}_p(t)$, is the velocity an exact nonlinearity compensation and decoupling control input will force the manipulator to follow (Horowitz and Tomizuka, 1980).

Defining the reference velocity error signal to be

$$\mathbf{e}_v(t) = \dot{\mathbf{x}}_p(t) - \mathbf{v}_p(t), \quad (3.3)$$

the control law which determines the actuator input is given by

$$\mathbf{q}(t) = \mathbf{W}(\mathbf{x}_p, \dot{\mathbf{x}}_p, \mathbf{v}_p, \mathbf{u})\hat{\boldsymbol{\Theta}}(t) - \mathbf{F}_v \mathbf{e}_v(t) - \mathbf{F}_p \mathbf{e}(t) + \mathbf{d}_m(\dot{\mathbf{x}}_p, \mathbf{q}), \quad (3.4)$$

where $\mathbf{W}(\mathbf{x}_p, \dot{\mathbf{x}}_p, \mathbf{v}_p, \mathbf{u})$ is defined by equation (2.9) and $\hat{\boldsymbol{\Theta}}(t)$ is an estimate of the parameter vector $\boldsymbol{\Theta}$. $\mathbf{F}_p = \sigma_p^2 \mathbf{I}_n$, \mathbf{I}_n is the $n \times n$ identity matrix¹ and \mathbf{F}_v is a positive definite gain matrix. We

define σ_v to be the minimum eigenvalue of $\mathbf{M}^{-\frac{T}{2}}(\mathbf{x}_p)\mathbf{F}_v\mathbf{M}^{-\frac{1}{2}}(\mathbf{x}_p)$

over all \mathbf{x}_p 's, where $\mathbf{M}(\mathbf{x}_p) = \mathbf{M}^{\frac{T}{2}}\mathbf{M}^{\frac{1}{2}}$.

Employing the control law given by equation (3.4) in the system given by equation (2.1) results in the following error dynamics:

¹The diagonal structure of \mathbf{F}_p is chosen for simplicity and poses no loss of generality in the analysis that follows.

$$\mathbf{M}(\mathbf{x}_p)\frac{D}{dt}\mathbf{e}_v = -\mathbf{F}_v\mathbf{e}_v - \mathbf{F}_p\mathbf{e} + \mathbf{w}_d \quad (3.5)$$

$$\frac{d}{dt}\mathbf{e} = \mathbf{e}_v - \lambda_p\mathbf{e},$$

where

$$\mathbf{w}_d = \mathbf{W}(\mathbf{x}_p, \dot{\mathbf{x}}_p, \mathbf{v}_p, \mathbf{u})\tilde{\boldsymbol{\Theta}} + \mathbf{d}_u(t), \quad \tilde{\boldsymbol{\Theta}} = \hat{\boldsymbol{\Theta}} - \boldsymbol{\Theta}. \quad (3.6)$$

As shown in Sadegh and Horowitz (1987b), the unperturbed closed-loop error system (i.e., $\mathbf{w}_d = 0$) given by equation (3.5) is globally exponentially stable, i.e., both $\mathbf{e}_v(t)$ and $\mathbf{e}(t)$ converge to zero exponentially from a given initial condition.

In order to implement the ECCL given by equation (3.4) above, it is necessary to calculate the elements of $\mathbf{W}(\mathbf{x}_p, \dot{\mathbf{x}}_p, \mathbf{v}_p, \mathbf{u})$ in real time. This procedure may be excessively time consuming, since it involves computations of highly nonlinear functions of joint positions and velocities. Consequently, the real time implementation of such a scheme may be difficult.

To overcome this difficulty we will now introduce several modifications to the control law in equation (3.4). The first modification consists of replacing \mathbf{x}_p by \mathbf{x}_d , $\dot{\mathbf{x}}_p$ and \mathbf{v}_p by $\dot{\mathbf{x}}_d$ and \mathbf{u} by $\ddot{\mathbf{x}}_d$ in the $\mathbf{W}(\mathbf{x}_p, \dot{\mathbf{x}}_p, \mathbf{v}_p, \mathbf{u})$ matrix. If the desired trajectory quantities, \mathbf{x}_d , $\dot{\mathbf{x}}_d$, and $\ddot{\mathbf{x}}_d$, are known in advance, the computation of the $\mathbf{W}(\mathbf{x}_d, \dot{\mathbf{x}}_d, \dot{\mathbf{x}}_d, \ddot{\mathbf{x}}_d)$ matrix can be performed off-line.

The second modification consists of introducing an additional nonlinear term, \mathbf{q}_n in the control law. This term will have the role of compensating for the additional error introduced in the manipulator dynamics due to replacement of \mathbf{x}_p , $\dot{\mathbf{x}}_p$, \mathbf{v}_p , and \mathbf{u} by their desired counterparts in the $\mathbf{W}(\mathbf{x}_p, \dot{\mathbf{x}}_p, \mathbf{v}_p, \mathbf{u})$ matrix.

The modified control law is given by:

$$\mathbf{q}(t) = \mathbf{W}(\mathbf{x}_d, \dot{\mathbf{x}}_d, \dot{\mathbf{x}}_d, \ddot{\mathbf{x}}_d)\hat{\boldsymbol{\Theta}} - \mathbf{F}_v\mathbf{e}_v - \mathbf{F}_p\mathbf{e} + \mathbf{d}_m(\dot{\mathbf{x}}_p, \mathbf{q}) - \mathbf{q}_n(\mathbf{e}_v, \mathbf{e}) \quad (3.7)$$

where

$$\mathbf{W}(\mathbf{x}_d, \dot{\mathbf{x}}_d, \dot{\mathbf{x}}_d, \ddot{\mathbf{x}}_d)\boldsymbol{\Theta} = \mathbf{M}(\mathbf{x}_d)\ddot{\mathbf{x}}_d + \mathbf{C}(\mathbf{x}_d, \dot{\mathbf{x}}_d)\dot{\mathbf{x}}_d + \mathbf{g}(\mathbf{x}_d) \quad (3.8)$$

and $\hat{\boldsymbol{\Theta}}$ is an estimate of $\boldsymbol{\Theta}$.

The nonlinear term, \mathbf{q}_n , is given by

$$\mathbf{q}_n(\mathbf{e}_v, \mathbf{e}) = \sigma_n |\mathbf{e}|^2 \mathbf{e}_v, \quad \sigma_n > 0 \quad (3.9)$$

This control law, which uses the desired trajectory quantities in the nonlinearity feed-forward compensation, will be referred to as the Desired Compensation Control Law (DCCL) in the remainder of this paper.

Applying the control law given by (3.7) to the manipulator (2.1), we obtain the following equation for the error dynamics:

$$\mathbf{M}(\mathbf{x}_p)\frac{D}{dt}\mathbf{e}_v = -\mathbf{F}_v\mathbf{e}_v - \mathbf{F}_p\mathbf{e} - \Delta\mathbf{W}(\mathbf{e}_v, \mathbf{e}) - \mathbf{q}_n + \mathbf{w}_d \quad (3.10)$$

$$\frac{d}{dt}\mathbf{e} = \mathbf{e}_v - \lambda_p\mathbf{e}$$

where

$$\mathbf{w}_d = \mathbf{W}(\mathbf{x}_d, \dot{\mathbf{x}}_d, \dot{\mathbf{x}}_d, \ddot{\mathbf{x}}_d)\tilde{\boldsymbol{\Theta}} + \mathbf{d}_u, \quad (3.11)$$

$$\Delta\mathbf{W}(\mathbf{e}_v, \mathbf{e}) = (\mathbf{W}(\mathbf{x}_p, \dot{\mathbf{x}}_p, \mathbf{v}_p, \mathbf{u}) - \mathbf{W}(\mathbf{x}_d, \dot{\mathbf{x}}_d, \dot{\mathbf{x}}_d, \ddot{\mathbf{x}}_d))\boldsymbol{\Theta}.$$

and \mathbf{d}_u are the unmodelled input disturbances to the manipulator.

As can be seen in equation (3.3), an additional term $\Delta\mathbf{W}(\mathbf{e}_v, \mathbf{e})$ is introduced. The following Lemma provides explicit bounds on $\Delta\mathbf{W}(\mathbf{e}_v, \mathbf{e})$.

(3.1) Lemma (Sadegh, Horowitz (1987b)): For the error system (3.10), the following equation holds

$$\Delta\mathbf{W}(\mathbf{e}_v, \mathbf{e}) = -\lambda_p\mathbf{M}(\mathbf{x}_p)\mathbf{e}_v + \lambda_p^2\mathbf{M}(\mathbf{x}_p)\mathbf{e} + \tilde{\Delta}\mathbf{W}(\mathbf{e}_v, \mathbf{e}) \quad (3.12)$$

where $\tilde{\Delta}\mathbf{W}(\mathbf{e}_v, \mathbf{e})$ satisfies the following inequality:

$$|\tilde{\Delta}\mathbf{W}(\mathbf{e}_v, \mathbf{e})| \leq b_1|\mathbf{e}_v| + b_2|\mathbf{e}| + b_3\left(|\mathbf{e}_v||\mathbf{e}| + \lambda_p|\mathbf{e}|^2\right). \quad (3.13)$$

$b_1, b_2,$ and b_3 in (3.13) are all bounded positive valued functions of $\dot{\mathbf{x}}_d$ and $\ddot{\mathbf{x}}_d$.

We now present the following stability theorem for the DCCL:

(3.2) Theorem (Sadegh, Horowitz (1987b)): For the error system governed by equations (3.10) and (3.11), under the conditions that $\sigma_v, \sigma_p,$ and σ_n are chosen sufficiently large, the unperturbed closed loop error system (i.e., $\mathbf{w}_d=0$) is globally exponentially stable, i.e., both $\mathbf{e}_v(t)$ and $\mathbf{e}(t)$ converge to zero exponentially from a given initial condition.

Proof

The proof of this theorem is based on the Lyapunov approach. Let us first define the maximum and minimum eigenvalues of \mathbf{M} :

$$\underline{\lambda}_m^2 = \inf_{x_p} \inf_{|v|=1} |\mathbf{M}(x_p)\mathbf{v}|, \quad \bar{\lambda}_m^2 = \sup_{x_p} \sup_{|v|=1} |\mathbf{M}(x_p)\mathbf{v}|, \quad (3.14)$$

and the generalized error state vector:

$$\bar{\mathbf{e}} = \begin{bmatrix} \bar{\mathbf{e}}_v \\ \bar{\mathbf{e}}_p \end{bmatrix} = \begin{bmatrix} \mathbf{M}^2 \mathbf{e}_v \\ \bar{\sigma}_p \mathbf{e} \end{bmatrix} \quad (3.15)$$

where

$$\bar{\sigma}_p^2 = \sigma_p^2 + \hat{\lambda}_m^2 \lambda_p^2, \quad \hat{\lambda}_m^2 = \frac{1}{2}(\underline{\lambda}_m^2 + \bar{\lambda}_m^2). \quad (3.16)$$

Defining the Lyapunov function candidate by

$$V(t, \bar{\mathbf{e}}) = \frac{1}{2} \bar{\mathbf{e}}^T \bar{\mathbf{e}} = \frac{1}{2} \mathbf{e}_v^T \mathbf{M}(\mathbf{e} + \mathbf{x}_d(t)) \mathbf{e}_v + \frac{1}{2} \bar{\sigma}_p^2 |\mathbf{e}|^2 \quad (3.17)$$

and utilizing the property of the covariant derivative given by equation (2.8), we obtain the following expression for the time derivative of the Lyapunov function candidate:

$$\begin{aligned} \frac{d}{dt} V(t, \bar{\mathbf{e}}) &= -\sigma_v |\bar{\mathbf{e}}_v|^2 - \lambda_p |\bar{\mathbf{e}}_p|^2 \\ &+ \lambda_p^2 \hat{\lambda}_m^2 \mathbf{e}_v^T \mathbf{e} - \mathbf{e}_v^T \Delta \mathbf{W}(\mathbf{e}_v, \mathbf{e}) - \mathbf{e}_v^T \mathbf{q}_n(\mathbf{e}_v, \mathbf{e}) \end{aligned} \quad (3.18)$$

Notice that $|\mathbf{M} - \hat{\lambda}_m^2 \mathbf{I}_n| \leq \left[\frac{\bar{\lambda}_m^2 - \underline{\lambda}_m^2}{2} \right]$. By using the expression for $\Delta \mathbf{W}(\mathbf{e}_v, \mathbf{e})$ from Lemma (3.1), the definition of $\mathbf{q}_n(\mathbf{e}_v, \mathbf{e})$ given in equation (3.9) and by choosing $\sigma_n \geq (1 + \lambda_p) b_3$, we obtain

$$\frac{d}{dt} V(t, \bar{\mathbf{e}}) \leq -[|\bar{\mathbf{e}}_v| \quad |\bar{\mathbf{e}}_p|] \mathbf{Q} \begin{bmatrix} |\bar{\mathbf{e}}_v| \\ |\bar{\mathbf{e}}_p| \end{bmatrix} \quad (3.19)$$

where

$$\mathbf{Q} = \begin{bmatrix} \bar{\sigma}_v & 0 \\ 0 & \lambda_p \end{bmatrix} + \bar{\mathbf{Q}} \quad (3.20)$$

and

$$\bar{\mathbf{Q}} = \begin{bmatrix} \bar{\sigma}_v - \lambda_p - \frac{b_3 + 4b_1}{4\underline{\lambda}_m^2} & \frac{b_2}{2\bar{\sigma}_p \underline{\lambda}_m} + \frac{\lambda_m \lambda_p^2}{2\bar{\sigma}_p} \left(\frac{\bar{\lambda}_m^2}{\underline{\lambda}_m^2} - 1 \right) \\ \frac{b_2}{2\bar{\sigma}_p \underline{\lambda}_m} + \frac{\lambda_m \lambda_p^2}{2\bar{\sigma}_p} \left(\frac{\bar{\lambda}_m^2}{\underline{\lambda}_m^2} - 1 \right) & \bar{\lambda}_p - \frac{\lambda_p b_3}{4\bar{\sigma}_p^2} \end{bmatrix} \quad (3.21)$$

Notice that in equations (3.20) and (3.21) we have decomposed σ_v and λ_p into:

$$\sigma_v = \bar{\sigma}_v + \tilde{\sigma}_v \quad \text{and} \quad \lambda_p = \bar{\lambda}_p + \tilde{\lambda}_p. \quad (3.22)$$

It is always possible to choose $\bar{\sigma}_v, \sigma_p,$ and λ_p such that, $\bar{\mathbf{Q}} \geq 0$. Thus,

$$\begin{aligned} \frac{d}{dt} V(t, \bar{\mathbf{e}}) &\leq -\bar{\sigma}_v \mathbf{e}_v^T \mathbf{M}(x_p) \mathbf{e}_v - \bar{\lambda}_p \mathbf{e}^T \mathbf{F}_p \mathbf{e} \\ &\leq -\gamma V(t, \bar{\mathbf{e}}) \leq 0 \quad \text{where} \quad \gamma = \min(\bar{\sigma}_v, \bar{\lambda}_p) \end{aligned} \quad (3.23)$$

Thus, both $\mathbf{e}_v(t)$ and $\mathbf{e}(t)$ converge to zero exponentially.

For the purpose of facilitating the analysis in subsequent sections, we will decompose the velocity feedback gain \mathbf{F}_v into

$$\mathbf{F}_v = \mathbf{F}_{v1} + \mathbf{F}_{v2} \quad (3.24)$$

such that $\mathbf{F}_{v1} > 0$ and \mathbf{F}_{v2} satisfies

$$\min_{x_p} \lambda(\mathbf{M}^{-\frac{T}{2}} \mathbf{F}_{v2} \mathbf{M}^{-\frac{1}{2}}) \geq \bar{\sigma}_v \quad (3.25)$$

$\bar{\sigma}_v > 0$ is sufficiently large so that $\bar{\mathbf{Q}} \geq 0$.

Utilizing equations (3.24) and (3.25), equation (3.23) can also be rewritten as follows:

$$\frac{d}{dt} V(t, \bar{\mathbf{e}}) \leq -\mathbf{e}_v^T \mathbf{F}_{v1} \mathbf{e}_v - \bar{\lambda}_p \mathbf{e}^T \mathbf{F}_p \mathbf{e}. \quad (3.26)$$

4 The Desired Compensation Adaptive Law (DCAL)

In the previous section, it was shown that, in order to achieve asymptotic convergence to zero of the extended error $\bar{\mathbf{e}}$, exact knowledge of $\mathbf{W}(x_p, \dot{x}_p, v_p, \mathbf{u})\Theta$ or $\mathbf{W}(x_d, \dot{x}_d, \ddot{x}_d)\Theta$ was required. In this section we will not assume any a priori knowledge of Θ . Thus, a parameter adaptation law will be introduced in order to estimate the parameter vector Θ on line. It will be shown that, under some mild conditions, the asymptotic stability properties of the fixed parameter controller still holds in the adaptive case.

The adaptive control law is the same as the DCCL, equation (3.4), with the difference that an adjustable $\hat{\Theta}$ is used as an estimate of the unknown parameter Θ .

$$\begin{aligned} \mathbf{q}(t) &= \mathbf{W}(x_d, \dot{x}_d, \ddot{x}_d)\hat{\Theta} - \mathbf{F}_v \mathbf{e}_v - \mathbf{F}_p \mathbf{e} \\ &+ \mathbf{d}_m(\dot{x}_p, \mathbf{q}) - \mathbf{q}_n(\mathbf{e}_v, \mathbf{e}) \end{aligned} \quad (4.1)$$

The following parameter adaptation algorithm is utilized to update the parameter estimate vector $\hat{\Theta}(t)$:

$$\frac{d}{dt} \hat{\Theta}(t) = -\Gamma \mathbf{W}^T(x_d, \dot{x}_d, \ddot{x}_d) \mathbf{e}_v(t), \quad \Gamma > 0 \quad (4.2)$$

where $\mathbf{W}(x_d, \dot{x}_d, \ddot{x}_d)$ was defined in equation (3.8).

Employing the control law given by equation (4.1) in the manipulator dynamic equation given by equation (2.1), we obtain the following error dynamics:

$$\begin{aligned} \mathbf{M}(x_p) \frac{d}{dt} \mathbf{e}_v &= -\hat{\mathbf{F}}_v \mathbf{e}_v - \mathbf{F}_p \mathbf{e} - \Delta \mathbf{W}(\mathbf{e}_v, \mathbf{e}) - \mathbf{q}_n + \mathbf{W}(x_d, \dot{x}_d, \ddot{x}_d) \tilde{\Theta} + \mathbf{d}_u \\ \frac{d}{dt} \mathbf{e} &= \mathbf{e}_v - \lambda_p \mathbf{e} \\ \frac{d}{dt} \tilde{\Theta} &= -\Gamma \mathbf{W}^T(x_d, \dot{x}_d, \ddot{x}_d) \mathbf{e}_v, \quad \Gamma > 0, \quad \tilde{\Theta} = \hat{\Theta} - \Theta, \end{aligned} \quad (4.3)$$

where

$$\Delta \mathbf{W}(\mathbf{e}_v, \mathbf{e}) = (\mathbf{W}(x_p, \dot{x}_p, v_p, \mathbf{u}) - \mathbf{W}(x_d, \dot{x}_d, \ddot{x}_d))\Theta. \quad (4.4)$$

Notice that the parameter adaptation law contains only the desired trajectory quantities in its adaptation signal. Therefore, the adaptation signal $\mathbf{W}(x_d, \dot{x}_d, \ddot{x}_d)$ may be calculated and stored off-line. Additionally, the adaptation law in equation (4.2) is more robust to stochastic disturbances than the adaptive version of the ECCL (i.e., utilizing $\mathbf{W}(x_p, \dot{x}_p, v_p, \mathbf{u})$ instead of $\mathbf{W}(x_d, \dot{x}_d, \ddot{x}_d)$). This results from the fact that the matrix $\mathbf{W}(x_d, \dot{x}_d, \ddot{x}_d)$ is not contaminated with noise, hence avoiding noise correlation between the error signal and the adaptation signal.

(2.2) Theorem: (Sadegh and Horowitz, (1987b)) For the unperturbed error dynamics governed by equation (4.3), i.e., $\mathbf{d}_u=0$, the following properties hold:

- (i) The error between the desired and actual trajectory converges asymptotically to zero, i.e., $\lim_{t \rightarrow \infty} [\mathbf{x}_d(t) - \mathbf{x}_p(t)] = 0$ and $\lim_{t \rightarrow \infty} [\dot{\mathbf{x}}_d(t) - \dot{\mathbf{x}}_p(t)] = 0$

(ii) If $\ddot{\mathbf{x}}_d(t)$ is uniformly continuous almost everywhere, then:

$$(a) \lim_{t \rightarrow \infty} \mathbf{W}(\mathbf{x}_d, \dot{\mathbf{x}}_d, \ddot{\mathbf{x}}_d) \bar{\Theta} = 0$$

(b) If in addition $\mathbf{W}(\mathbf{x}_d, \dot{\mathbf{x}}_d, \ddot{\mathbf{x}}_d)$ is persistently exciting then:

$$\lim_{t \rightarrow \infty} \bar{\Theta}(t) = 0$$

Proof: See Sadegh and Horowitz (1987b).

5 Repetitive Control Law (RCL)

In this section we will consider the control of robotic manipulators for repetitive tasks. By a repetitive task we mean that the robot is required to execute the same motion over and over again with a fixed periodicity. Therefore, for these applications, it is assumed that the desired trajectory signals, $\mathbf{x}_d(t)$, $\dot{\mathbf{x}}_d(t)$, and $\ddot{\mathbf{x}}_d(t)$ are periodic and bounded. Namely,

$$\mathbf{x}_d(t+T) = \mathbf{x}_d(t), \dot{\mathbf{x}}_d(t+T) = \dot{\mathbf{x}}_d(t), \ddot{\mathbf{x}}_d(t+T) = \ddot{\mathbf{x}}_d(t) \quad (5.1)$$

where T is the period.

An immediate consequence of equation (5.1) is that the term $\mathbf{W}(\mathbf{x}_d, \dot{\mathbf{x}}_d, \ddot{\mathbf{x}}_d) \bar{\Theta}$ is also periodic. We will denote this periodic term by $\mathbf{w}_r(t)$ and assume that its lower and upper bounds are known for all $t \in [0, T]$.

$$\mathbf{w}_r(t) = \mathbf{W}(\mathbf{x}_d, \dot{\mathbf{x}}_d, \ddot{\mathbf{x}}_d) \bar{\Theta}, \quad (5.2)$$

$$\mathbf{w}_r(t+T) = \mathbf{w}_r(t)$$

and

$$\underline{\mathbf{w}}_{r_i} < \mathbf{w}_{r_i}(t) < \bar{\mathbf{w}}_{r_i}, \text{ for all } t, \quad (5.3a)$$

where $\bar{\mathbf{w}}_{r_i}$ and $\underline{\mathbf{w}}_{r_i}$ are the known upper and lower bounds of $\mathbf{w}_{r_i}(t)$, and

$$\max\{|\mathbf{w}_r - \underline{\mathbf{w}}_{r_i}|, |\bar{\mathbf{w}}_{r_i} - \mathbf{w}_r|\} < r_w \quad (5.3b)$$

The repetitive control law is given by:

$$\mathbf{q}(t) = \hat{\mathbf{w}}_r(t) - \mathbf{F}_v \mathbf{e}_v - \mathbf{F}_p \mathbf{e} + \mathbf{d}_m(\dot{\mathbf{x}}_p, \mathbf{q}) - \mathbf{q}_n(\mathbf{e}_v, \mathbf{e}) \quad (5.4)$$

where the term $\hat{\mathbf{w}}_r(t)$ is an estimate of the periodic function $\mathbf{w}_r(t)$, and all other terms in equation (5.4) are defined in equations (3.4) or (3.7).

The following ‘learning’ algorithm is proposed for updating the estimate $\hat{\mathbf{w}}_r(t)$:

$$\hat{\mathbf{w}}_r^*(t) = \hat{\mathbf{w}}_r(t-T) - \mathbf{K}_L \mathbf{e}_v(t), \mathbf{K}_L > 0 \quad (5.5a)$$

$$\hat{\mathbf{w}}_r(t) = \pi(\hat{\mathbf{w}}_r^*(t)) \quad (5.5b)$$

where $\pi(\bullet)$ is the projection given by the following equation:

$$\pi(\hat{\mathbf{w}}_r^*) = \begin{cases} \hat{\mathbf{w}}_r^*(t) & \text{if } \mathbf{w}_{r_i}(t) - \delta \leq \hat{\mathbf{w}}_r^*(t) \leq \bar{\mathbf{w}}_{r_i}(t) + \delta \\ \mathbf{w}_{r_i}(t) & \text{if } \hat{\mathbf{w}}_r^*(t) < \mathbf{w}_{r_i}(t) - \delta \\ \bar{\mathbf{w}}_{r_i}(t) & \text{if } \hat{\mathbf{w}}_r^*(t) > \bar{\mathbf{w}}_{r_i}(t) + \delta \end{cases} \quad (5.6)$$

and $\delta > 0$ is a small arbitrary constant.

Employing the control law given by equations (5.4)–(5.6) in the manipulator dynamic equation given by equation (2.1), the following error dynamic equation is obtained:

$$\mathbf{M}(\mathbf{x}_p) \frac{D}{dt} \mathbf{e}_v = -\mathbf{F}_v \mathbf{e}_v - \mathbf{F}_p \mathbf{e} - \Delta \mathbf{W}(\mathbf{e}_v, \mathbf{e}) - \mathbf{q}_n + \tilde{\mathbf{w}}_r(t) + \mathbf{d}_u \quad (5.7)$$

$$\frac{d}{dt} \mathbf{e} = \mathbf{e}_v - \lambda_p \mathbf{e}$$

where

$$\Delta \mathbf{W}(\mathbf{e}_v, \mathbf{e}) = (\mathbf{W}(\mathbf{x}_p, \dot{\mathbf{x}}_p, \mathbf{v}_p, \mathbf{u}) - \mathbf{W}(\mathbf{x}_d, \dot{\mathbf{x}}_d, \ddot{\mathbf{x}}_d)) \bar{\Theta}. \quad (5.8)$$

and

$$\tilde{\mathbf{w}}_r(t) = \hat{\mathbf{w}}_r(t) - \mathbf{w}_r(t). \quad (5.9)$$

Notice that the structure of the repetitive control in equation (5.4) is very similar to that of the adaptive controller given in equation (4.1), with the difference that the ‘learning’ algorithm given by equations (5.5) and (5.6) is used instead of the adaptation algorithm in equation (4.2). Therefore, it is not

surprising that the error dynamics in equations (5.7)–(5.9) is very similar in structure to that of equations (4.3) and (4.4).

(5.1) Theorem: Assuming that the signal $\mathbf{w}_r(t)$ is both periodic and bounded, with known period T and with known lower and upper bounds $\underline{\mathbf{w}}_r(t)$ and $\bar{\mathbf{w}}_r(t)$, respectively; for the unperturbed error dynamics governed by equations (5.7)–(5.9), i.e., $\mathbf{d}_u = 0$, and utilizing the ‘learning’ algorithm given by equations (5.5) and (5.6), the following property holds:

The error between the desired and actual trajectory converges to zero asymptotically, i.e.

$$\lim_{t \rightarrow \infty} [\mathbf{x}_d(t) - \mathbf{x}_p(t)] = 0 \text{ and } \lim_{t \rightarrow \infty} [\dot{\mathbf{x}}_d(t) - \dot{\mathbf{x}}_p(t)] = 0$$

Proof

The proof of this theorem will be carried out in a similar manner to the proof of Theorem (3.2). We will utilize the definition of the generalized error state vector, $\bar{\mathbf{e}}$, in equations (3.15) and (3.16), and define the following Lyapunov functional candidate.

$$V(t, \bar{\mathbf{e}}) = \frac{1}{2} \bar{\mathbf{e}}^T \bar{\mathbf{e}} + \frac{1}{2} \int_{t-T}^t \tilde{\mathbf{w}}_r^T(\tau) \mathbf{K}_L^{-1} \tilde{\mathbf{w}}_r(\tau) d\tau \quad (5.10)$$

Notice that the Lyapunov functional in equation (5.10) is the same as the Lyapunov function in equation (3.17), with an additional integral term.

Differentiating equation (5.10) with respect to time, and taking into account the results obtained in the proof of Theorem (3.2), we obtain:

$$\frac{d}{dt} V(t, \bar{\mathbf{e}}) \leq -\mathbf{e}_v^T \mathbf{F}_v \mathbf{e}_v - \bar{\lambda}_p \mathbf{e}^T \mathbf{F}_p \mathbf{e} + \mathbf{e}_v^T \tilde{\mathbf{w}}_r(t) \quad (5.11)$$

$$+ \frac{1}{2} [\tilde{\mathbf{w}}_r^T(t) \mathbf{K}_L^{-1} \tilde{\mathbf{w}}_r(t) - \tilde{\mathbf{w}}_r^T(t-T) \mathbf{K}_L^{-1} \tilde{\mathbf{w}}_r(t-T)],$$

where the last term in equation (5.11) results from the differentiation of the integral term in the Lyapunov function.

We will now consider two cases:

Case *i*: $\underline{\mathbf{w}}_{r_i} - \delta \leq \hat{\mathbf{w}}_r^*(t) \leq \bar{\mathbf{w}}_{r_i} + \delta$ for all i .

In this case, from equations (5.3), (5.5) and (5.9)

$$\mathbf{e}_v^T \tilde{\mathbf{w}}_r(t) = -\frac{1}{2} [\tilde{\mathbf{w}}_r^T(t) \mathbf{K}_L^{-1} \tilde{\mathbf{w}}_r(t) - \tilde{\mathbf{w}}_r^T(t-T) \mathbf{K}_L^{-1} \tilde{\mathbf{w}}_r(t-T)] - \frac{1}{2} \mathbf{e}_v^T(t) \mathbf{K}_L \mathbf{e}_v(t). \quad (5.12)$$

Thus,

$$\frac{d}{dt} V(t, \bar{\mathbf{e}}) \leq -\mathbf{e}_v^T \left[\mathbf{F}_v + \frac{1}{2} \mathbf{K}_L \right] \mathbf{e}_v - \bar{\lambda}_p \mathbf{e}^T \mathbf{F}_p \mathbf{e} \leq 0. \quad (5.13)$$

Case *ii*: $\hat{\mathbf{w}}_r^*(t) < \underline{\mathbf{w}}_{r_i}(t) - \delta$ or $\hat{\mathbf{w}}_r^*(t) > \bar{\mathbf{w}}_{r_i}(t) + \delta$ for some i .

In this case, if we allowed $\hat{\mathbf{w}}_r(t)$ to be equal to $\hat{\mathbf{w}}_r^*(t)$ then

$\frac{d}{dt} V(t, \bar{\mathbf{e}}) \leq 0$ as in equation (5.13) above. However, notice that since $\underline{\mathbf{w}}_{r_i}(t) \leq \mathbf{w}_{r_i}(t) \leq \bar{\mathbf{w}}_{r_i}(t)$,

$$|\hat{\mathbf{w}}_r(t) - \mathbf{w}_r(t)|^2 \leq |\hat{\mathbf{w}}_r^*(t) - \mathbf{w}_r(t)|^2. \quad (5.14)$$

Hence the Lyapunov functional does not increase after applying the projection algorithm given by equation (5.6).

Thus,

$$\lim_{t \rightarrow \infty} V(t) = V_{ss} < \infty \quad (5.15)$$

As a result, the extended error state, $\bar{\mathbf{e}}$, is bounded and, moreover, it is squared integrable (ϵL_2). Also, from boundedness

of $\tilde{\mathbf{w}}_r$, it follows, from equation (5.7), that $\frac{d}{dt} \bar{\mathbf{e}}$ is bounded

which implies the uniform continuity of $\|\bar{\mathbf{e}}\|^2$. The asymptotic convergence to zero of the position and the velocity tracking error, \mathbf{e} and \mathbf{e}_v , immediately follows from Barlat's Lemma (see Narendra and Valavani (1980)).

Remark 1: The projection algorithm (5.6) in the “learning” law in equation (5.5) was utilized in order to guarantee the boundness of the repetitive estimate $\hat{\mathbf{w}}_r(t)$. Notice however that, from the definition of the Lyapunov function candidate, $V(t)$, in equation (5.10), the boundedness of the position tracking error, \mathbf{e} and of the integral term

$$\frac{1}{2} \int_{t-T}^t \tilde{\mathbf{w}}_r^T(\tau) \mathbf{K}_L^{-1} \tilde{\mathbf{w}}_r(\tau) d\tau$$

is guaranteed without the necessity of the projection algorithm.

Remark 2: In actual implementations the “learning” law in equation (5.5) should be modified by including a dead-zone to improve the robustness of the algorithm to noise disturbances as follows:

$$\hat{\mathbf{w}}_r^*(t) = \hat{\mathbf{w}}_r(t-T) - \mathbf{K}_L \mathbf{e}_v(t), \mathbf{K}_L > 0 \quad (5.19)$$

$$\hat{\mathbf{w}}_r(t) = \begin{cases} \hat{\mathbf{w}}_r^*(t) & \text{if } \underline{\mathbf{w}}_r(t) \leq \hat{\mathbf{w}}_r^*(t) \leq \overline{\mathbf{w}}_r(t) \text{ and } |\mathbf{e}_v(t)| \geq \epsilon \\ \underline{\mathbf{w}}_r(t) & \text{if } \hat{\mathbf{w}}_r^*(t) < \underline{\mathbf{w}}_r(t) \text{ and } |\mathbf{e}_v(t)| \geq \epsilon \\ \overline{\mathbf{w}}_r(t) & \text{if } \hat{\mathbf{w}}_r^*(t) > \overline{\mathbf{w}}_r(t) \text{ and } |\mathbf{e}_v(t)| \geq \epsilon \\ \hat{\mathbf{w}}_r(t-T) & \text{if } |\mathbf{e}_v(t)| < \epsilon \end{cases}$$

where ϵ is width of the learning dead-zone. Notice that with this modification, the convergence to zero of the extended error state, $\bar{\mathbf{e}}$, is no longer guaranteed, however $|\bar{\mathbf{e}}|$ can be made arbitrarily small by making ϵ arbitrarily small.

6 Discrete Time Implementation-Hybrid Repetitive Control Law (HRCL)

The repetitive controller presented in the previous section is a continuous time controller. In the stability analysis presented in the previous sections, it was assumed that the estimate of the repetitive signal, $\hat{\mathbf{w}}_r(t)$ is updated continuously in time. Although the implementation of such controllers is certainly possible utilizing analog magnetic recording and playback equipment, it is of practical interest to explore the implementation of repetitive control laws utilizing digital computers. In this context the repetitive “learning” algorithm can no longer be analyzed as a continuous time algorithm, but rather as a discrete time algorithm. The control algorithm considered in this section is not fully a discrete time controller; only computationally or memory intensive operations in the control algorithm are implemented in discrete time. Thus, the controller is of hybrid nature.

In the discussion to be presented we will assume that the desired trajectory period, T is known, and is an integer multiple of the discrete time controller sampling time, Δt , i.e.,

$$T = N \Delta t \quad (6.1)$$

where N is the total number of controller samples occurring during the period T . We will also define the *sampling index* k and the *learning cycle index* j such that, for any time $t_{jk} > 0$, which is a multiple integer of Δt , the integers j and k are uniquely defined by

$$t_{jk} = jT + k\Delta t \quad j \geq 0 \text{ and } N \geq k \geq 0. \quad (6.2)$$

Consider the following repetitive control law.

$$\mathbf{q}(t) = \hat{\mathbf{w}}_r(t) - \mathbf{F}_v \mathbf{e}_v - \mathbf{F}_p \mathbf{e} + \mathbf{d}_m(\dot{\mathbf{x}}_p, \mathbf{q}) - \mathbf{q}_n(\mathbf{e}_v, \mathbf{e}) \quad (6.3)$$

where all terms in equation (6.3) have been previously defined, except that the estimate $\hat{\mathbf{w}}_r(t)$ in this case is updated by the following discrete time “learning algorithm”:

$$\hat{\mathbf{w}}_r(t) = \begin{cases} \hat{\mathbf{w}}_d(j, k-1) & \text{if } t_{jk} > t \geq t_{j(k-1)} \\ \hat{\mathbf{w}}_d(j, k) & \text{if } t = t_{jk} \end{cases} \quad (6.4)$$

$$\hat{\mathbf{w}}_d^*(j, k) = \hat{\mathbf{w}}_d(j-1, k) - \mathbf{K}_L \mathbf{e}_v^*(j-1, k) \quad (6.5)$$

$$\mathbf{e}_v^*(j, k) = \int_{t_{jk}}^{t_{j(k+1)}} \mathbf{e}_v(\tau) d\tau \quad (6.6a)$$

$$\mathbf{e}^{*2}(t) = \mathbf{e}_v^T \mathbf{e}_v(t) + \kappa_p \mathbf{e}^T \mathbf{F}_p \mathbf{e}(t), \quad \kappa_p > 0 \quad (6.6b)$$

$$\bar{\mathbf{e}}^{*2}(j, k) = \int_{t_{jk}}^{t_{j(k+1)}} \mathbf{e}^{*2}(\tau) d\tau \quad (6.6c)$$

and

$$\hat{\mathbf{w}}_d(j, k) = \begin{cases} \pi(\hat{\mathbf{w}}_d^*(j, k)) & \text{if } \bar{\mathbf{e}}^{*2}(j-1, k) > \epsilon^2 \Delta t \\ \hat{\mathbf{w}}_d(j-1, k) & \text{if } \bar{\mathbf{e}}^{*2}(j-1, k) \leq \epsilon^2 \Delta t \end{cases} \quad (6.7)$$

where $\pi(\cdot)$ is the projection law in equation (5.6), and ϵ^2 is the width of the learning dead zone, which will be subsequently defined. κ_p in equation (6.6b) is given by $\kappa_p = \frac{\bar{\lambda}_p}{\lambda_v}$, where $\bar{\lambda}_p$ is a term of the minor velocity loop gain, λ_p , as defined in equation (3.22) and λ_v will be subsequently defined by equation (6.13).

The signal $\mathbf{e}_v^*(j, k)$ can be interpreted as the average of the reference velocity error signal, \mathbf{e}_v , during the sampling interval $[t_{jk}, t_{j(k+1)}]$. Notice that, in order for the discrete time “learning” algorithm in equation (6.5) to be causal, the signal $\mathbf{e}_v^*(j-1, k)$ of the *previous* learning cycle $j-1$ is utilized in the computation of $\hat{\mathbf{w}}_d^*(j, k)$.

In order to analyze the stability of the HRCL, we need to define the sampled value of the repetitive signal $\mathbf{w}_r(t)$ at the instant t_{jk} ,

$$\mathbf{w}_d(k) = \mathbf{w}_r(t_{jk}) = \mathbf{w}_r(t_{(j+1)k}), \quad N \geq k \geq 0, \quad (6.8)$$

the sampled repetitive signal error sequence

$$\tilde{\mathbf{w}}_d(j, k) = \mathbf{w}_d(k) - \hat{\mathbf{w}}_d(j, k) \quad (6.9)$$

and the repetitive signal discretization error function

$$\Delta \mathbf{w}_d(t) = \mathbf{w}_r(t) - \mathbf{w}_r(t_{jk}), \quad \overline{\Delta \mathbf{w}_d} = \max_{t \in [0, T]} |\Delta \mathbf{w}_d(t)|, \quad (6.10)$$

where $\overline{\Delta \mathbf{w}_d}$ is the upper bound of the error introduced in the discretization of the repetitive signal $\mathbf{w}_r(t)$.

We define the Lyapunov sequence

$$V(j, k) = \frac{1}{2} \bar{\mathbf{e}}^T(t_{jk}) \bar{\mathbf{e}}(t_{jk}) + \frac{1}{2} \sum_{s=k}^{s=N} \tilde{\mathbf{w}}_d^T(j, s) \mathbf{K}_L^{-1} \tilde{\mathbf{w}}_d(j, s) + \frac{1}{2} \sum_{s=0}^{s=k-1} \tilde{\mathbf{w}}_d^T(j+1, s) \mathbf{K}_L^{-1} \tilde{\mathbf{w}}_d(j+1, s) \quad (6.11)$$

and the sequence

$$\Delta V(j, k) = \begin{cases} V(j, k+1) - V(j, k) & \text{for } N > k \geq 0 \\ V(j+1, 0) - V(j, N) & \text{for } k = N \end{cases} \quad (6.12)$$

for $j \geq 0$.

We also need to define the following quantities, which we will use in the sequel:

$$\lambda_v := \sigma_{\min}(\mathbf{F}_{v1} - \frac{1}{2} \Delta t \mathbf{K}_L) > 0 \quad (6.13)$$

$$\rho := \max \left\{ \frac{\bar{\lambda}_m}{\lambda_v}, \frac{1}{\lambda_p} \right\} \quad (6.14)$$

$$\epsilon^2 := \left[\frac{\overline{\Delta \mathbf{w}_d}}{\lambda_v} \right]^2, \quad (6.15)$$

where $\overline{\Delta \mathbf{w}_d}$ is defined in equation (6.10).

(6.1) Theorem: Consider the manipulator repetitive control law, given by equations (6.3)–(6.7), along with the hypothesis of theorem (5.1), then we conclude that all the error signals; \mathbf{e}_v , \mathbf{e} and $\tilde{\mathbf{w}}_d$; remain bounded. Moreover,

$$\lim_{j \rightarrow \infty} \bar{\mathbf{e}}^{*2}(t_{jk}) \leq \beta_1 \epsilon^2 + \beta_2 \epsilon, \quad (6.16)$$

where $\bar{\lim}$ denotes the upper limit, and

$$\beta_1 = 2(\rho + \sqrt{\rho \Delta t} + \Delta t), \quad \beta_2 = \frac{2r_w \sqrt{\rho \Delta t}}{\lambda_v}. \quad (6.17)$$

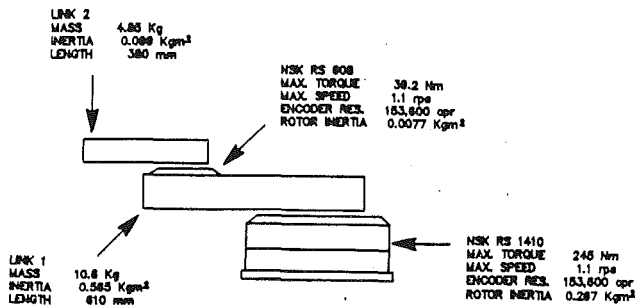


Fig. 1 NSK direct drive SCARA arm

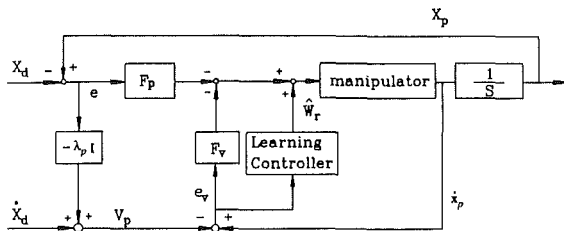


Fig. 2 Repetitive control system block diagram

We use the following notation for all the sampled sequences in the proof.

$$s(i) := s(t_i) = s(t_{jk}),$$

where $i = jN + k$. Also, we will use the following lemma in the proof of the theorem.

(6.2) **Lemma:** Given the hypothesis of the theorem (6.1), we assert:

$$(i) \bar{e}^{*2}(i) > \epsilon^2 \Delta t \rightarrow \Delta V(i) \leq -\frac{\lambda_v}{2} (\bar{e}^{*2} - \epsilon^2 \Delta t),$$

$$(ii) \bar{e}^{*2}(i) \leq \epsilon^2 \Delta t \text{ (for all } k < i < j) \rightarrow V(j) - V(k) \leq \alpha_1 \epsilon^2 + \alpha_2 \epsilon,$$

where

$$\alpha_1 = (\rho + \sqrt{\rho \Delta t}) \lambda_v, \quad \alpha_2 = \sqrt{\rho \Delta t} r_w$$

Proof: See Appendix.

Proof of Theorem (6.1)

The proof proceeds by contradiction. We assume that there exists a $\delta > 0$ such that for all k there exist an $i > k$ such that

$$\bar{e}^{*2}(i) > \beta_1 \epsilon^2 + \beta_2 \epsilon + \delta.$$

It is straightforward to see that there exists a sub-sequence of the sampled sequence, denoted by $\{p_i\}$, such that:

$$(i) \bar{e}^{*2}(p_i) > \beta_1 \epsilon^2 + \beta_2 \epsilon + \delta$$

(ii) There exist p_i^+ and p_{i+1}^- such that $p_i < p_i^+ + 1 \leq p_i^+ < p_{i+1}^- \leq p_{i+1}$ with $\bar{e}^{*2}(l) \leq \epsilon^2 \Delta t$ for all $p_i^+ \leq l < p_{i+1}^-$. Otherwise, the Lyapunov function decreases indefinitely, which is a contradiction.

$$(iii) V(p_i^+) - V(p_{i+1}) \leq 0$$

$$(iv) V(p_{i+1}) - V(p_{i+1}^-) \leq 0$$

Since $\bar{e}^{*2}(p_i) > \beta_1 \epsilon^2 + \beta_2 \epsilon + \delta$, plugging in the values of β_1 and β_2 , from Part (i) of lemma (6.2), we note that:

$$V(p_i + 1) - V(p_i) \leq -\alpha_1 \epsilon^2 - \alpha_2 \epsilon - \frac{1}{2} \lambda_v \delta \quad (6.18)$$

Part (ii) of lemma (6.2) implies that

$$V(p_{i+1}^-) - V(p_i^+) \leq \alpha_1 \epsilon^2 + \alpha_2 \epsilon \quad (6.19)$$

Adding equations (6.18)–(6.19) together and using (iii) and (iv), we obtain

$$V(p_{i+1}) - V(p_i) \leq -\frac{1}{2} \delta \lambda_v \quad (6.20)$$

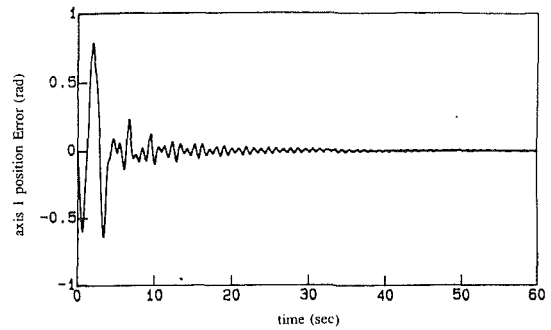


Fig. 3 Axis 1 position error

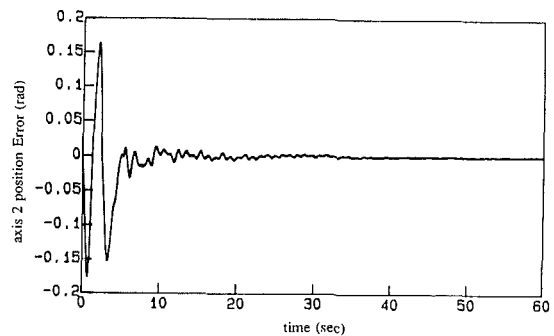


Fig. 4 Axis 2 position error

Thus, we conclude that $V(p_n) \leq V(p_0) - \frac{n}{2} \delta \lambda_v$ for all n , which is a contradiction since V has to remain positive for all times. We now complete the proof by the following argument: boundedness of \bar{e}^{*2} implies boundedness of $\int_{t_{jk}}^{t_{j(k+1)}} \bar{e}^T \bar{e}(\tau) d\tau$; using lemma (A.1) of the Appendix, we may conclude that \bar{e} is bounded for all times. In fact, it can be shown that the upper limit of $\bar{e}(t)$ converges to zero as ϵ converges to zero.

7 Simulation

A model of a two degrees of freedom SCARA type robot arm was used in the simulation study to investigate the performance of the proposed algorithm. See Fig. 1 for the configuration and corresponding parameters of the arm. The model is that of the Berkeley/NSK direct drive SCARA manipulator. The complete model description, which includes the nonlinear manipulator dynamics, as well as other nonlinearities, such as actuator saturation and Coulomb friction, and actuator and sensor parasitic dynamics can be found in Kang et al. (1988).

Figure 2 shows the block diagram for the overall control system. The control gains used for both axes in the simulations are as follows: $F_v = 40\mathbf{I}$; $F_p = 20\mathbf{I}$; and $\sigma_n = 10$. The repetitive gain, K_L , is 40. The desired position trajectory for both axes is $x_{d1} = x_{d2} = 2.5 - 2.5 \cos\left(\frac{2\pi t}{T}\right)$, where period T is taken to be

3 seconds. For the hybrid control, we used 10 millisecond for updating the repetitive control algorithm, and 1 microsecond as the integration step size for emulating the continuous torque input. The sinusoidal desired trajectories will produce a smooth desired repetitive input $\mathbf{W}(x_d, \dot{x}_d, \ddot{x}_d, \ddot{x}_d)$.

Figures 3–8 show the simulation results for both axes. The position and velocity errors as well as the errors between the (discretized) desired repetitive input and the actual adapting repetitive input for both axes converge to negligible values. The simulation shows very fast convergence for the first few periods. When the errors become smaller, the rate of convergence also slows down. This seems to be a common phenom-

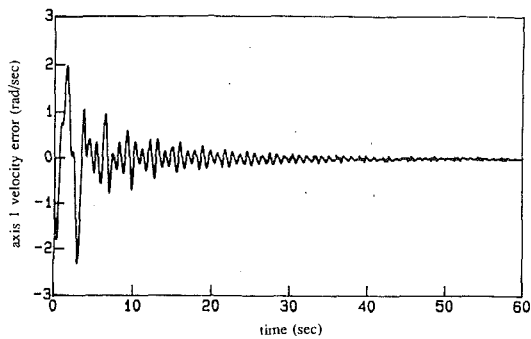


Fig. 5 Axis 1 auxiliary velocity error

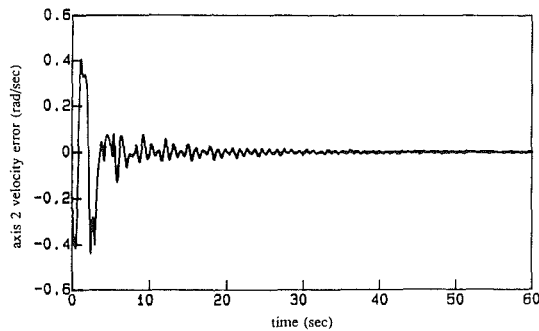


Fig. 6 Axis 2 auxiliary velocity error

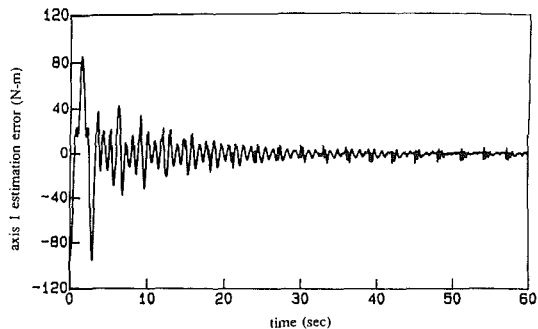


Fig. 7 Axis 1 feedforward estimation error ($W_{r1} - W_{d1}$)

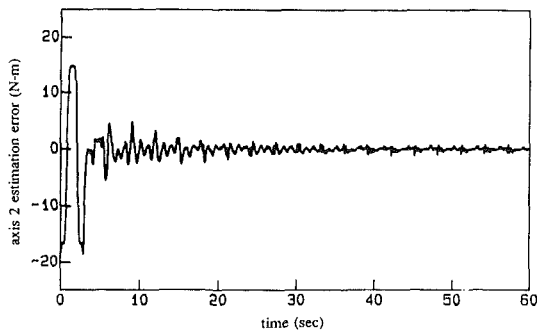


Fig. 8 Axis 2 feedforward estimation error ($W_{r2} - W_{d2}$)

enon when gradient estimation algorithms, such as the ones presented in this paper, are used in repetitive control schemes.

8 Real-Time Implementation

The repetitive control algorithm was also implemented digitally using the Berkeley/NSK direct drive SCARA manipulator, and an IBM PC AT equipped with an Amadeus-96 single board controller from Integrated Motions Inc. The details of the experimental setup can be found in Horowitz et al. (1989). The desired trajectories chosen for the experiments correspond to a typical pick and place task. A plot of the desired joint

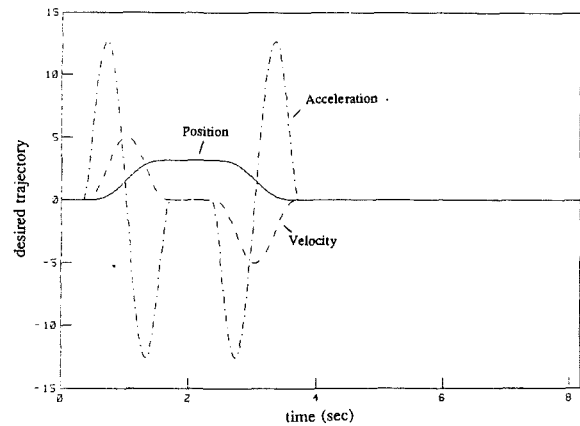


Fig. 9 Desired trajectory for implementations

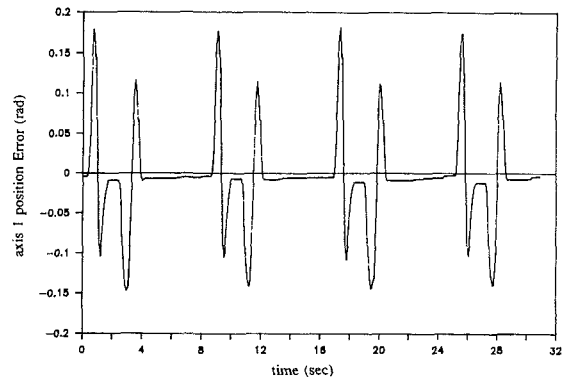


Fig. 10(a) PD control implementation results — axis 1

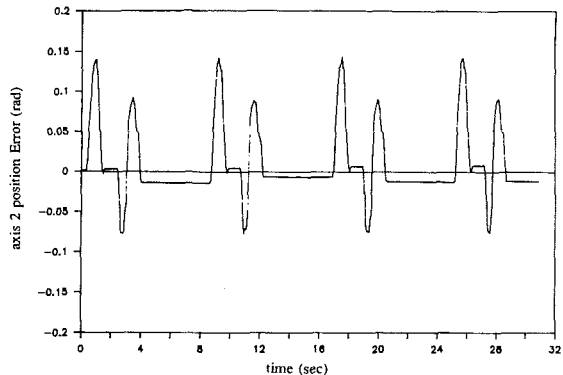


Fig. 10(b) PD control implementation results — axis 2

position, velocity and acceleration trajectories for both axes is shown in Fig. 9.

For comparison purposes, a PD controller was first implemented. The PD control gains for axes 1 and 2 were $F_{p1} = 200$, $F_{v1} = 120$, $F_{p2} = 20$, and $F_{v2} = 12$, respectively. The feedback controller sampling time was 2 ms using the Amadeus-96 board with integer math. The desired trajectories were updated every 8 ms. The results are shown in Fig. 10. Notice that friction compensation is not used in the actual implementations, hence the tracking errors are mostly due to friction forces at steady state. The error patterns are generally repetitive for both joints, with some slight variations in the extreme errors, and the steady-state errors caused by stiction.

In the case of the repetitive algorithm implementation, a 2 ms sampling time was used for the PD control, while the repetitive compensation was updated every 8 ms. Simulation and experimental results are shown in Fig. 11 and Fig. 12, respectively. As shown in Fig. 12, the tracking error during the first cycle is exactly the same as when PD control alone is

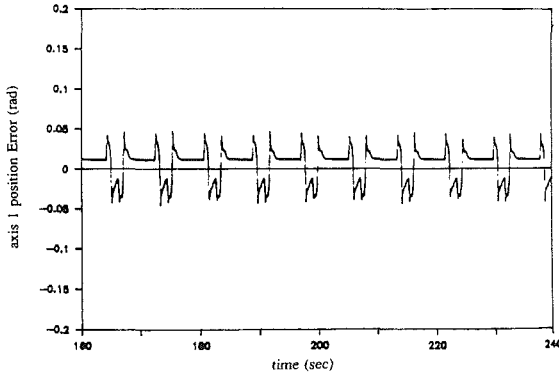
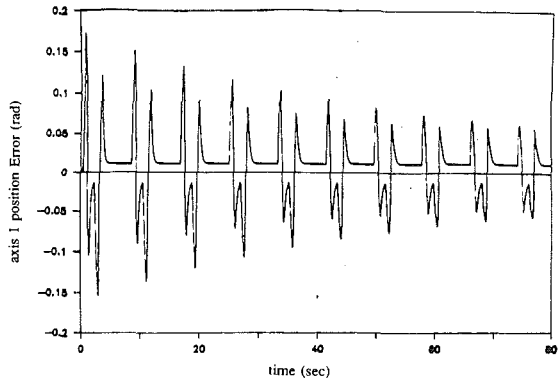


Fig. 11(a) Repetitive control simulation results — axis 1

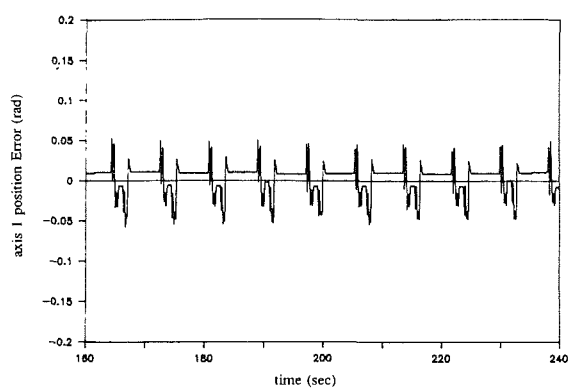
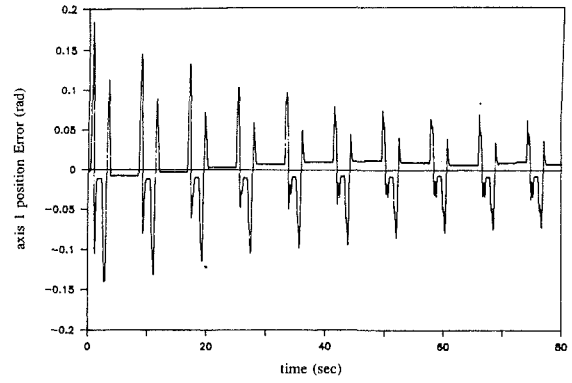


Fig. 12(a) Repetitive control implementation results — axis 1

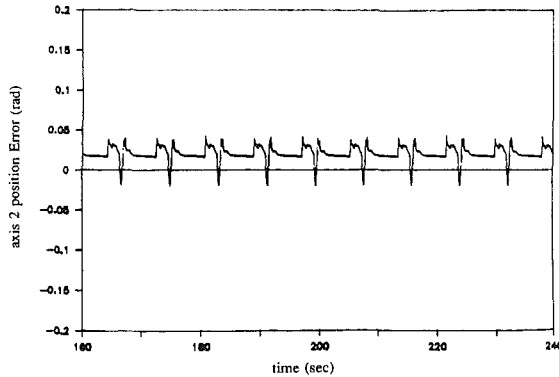
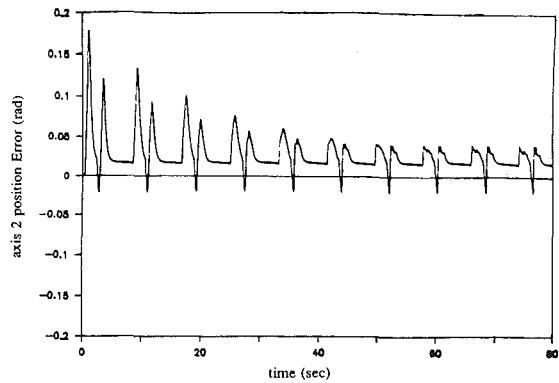


Fig. 11(b) Repetitive control simulation results — axis 2

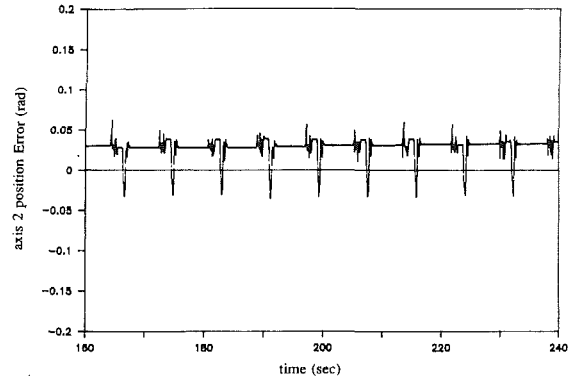
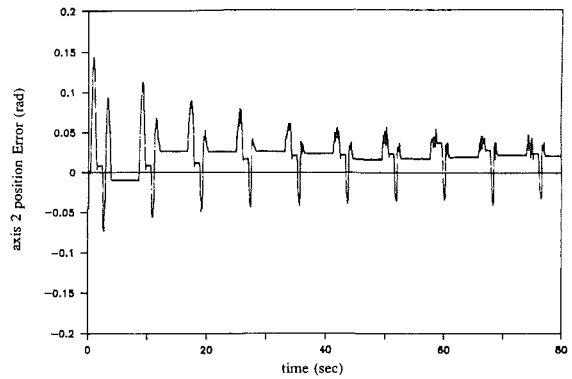


Fig. 12(b) Repetitive control implementation results — axis 2

utilized. However, the error decreases to within the deadzone once the learning action takes place. The deadzone size was 0.05 rad, which is a function of the control sampling rate. Due to the slow PD control sampling rate, the resulting tracking errors are significantly larger than the errors with continuous PD control. However, the repetitive compensation still reduces the tracking error by 75 percent.

9 Conclusions

Several adaptive and repetitive control algorithms for the trajectory following of robot manipulators were presented. Although different in appearance, both the adaptive and the repetitive schemes were shown to have similar characteristics

which allowed us to analyze them uniformly. In fact, a unified Lyapunov based technique was developed for synthesis and stability analysis of both schemes, which utilizes the passivity properties of robot manipulators. A complete stability proof was also presented for a proposed hybrid version of the repetitive control scheme.

Simulation studies and real-time implementations were conducted to evaluate the performance of the repetitive controller. Simulation results showed that the continuous time repetitive controller forces all errors to zero, as asserted in the corresponding theorems. The discretization of the algorithms in general prohibit complete elimination of the tracking errors. Real-time results are in close agreement with the theory and show that the tracking errors are reduced to within the pre-specified deadzone size.

The repetitive controller is recommended when the desired trajectory is periodic. In such applications, the repetitive control scheme provides a very simple adaptation algorithm and is very effective in removing any periodic tracking errors. The error convergence rate of repetitive algorithm, however, is slower than that of adaptive controllers (see Sadegh and Horowitz (1987b) for the adaptive controller simulation results). It also exhibits less robustness to noise disturbances. Adaptive controllers, on the other hand, may be used for more general trajectories, but explicit information of the manipulator model structure is required in the algorithm formulation. For tasks in which the desired trajectory contains both periodic and non-periodic signals, a combination of adaptive and repetitive controller may be utilized.

Acknowledgment

This work was supported by the National Science Foundation under grant MSM-8511955.

References

An, C. H., Atkeson, C. G., and Hollerbach, J. M., 1985, "Estimation of Inertial Parameters of Rigid Body Links of Manipulators," *Proc. 24th Conf. on Decision and Control*, Fort Lauderdale, Fla., Dec. 11-13, 1985.

Arimoto, S., Kawamura, S., Miyazaki, F., and Tamaki, S., 1985, "Learning Control Theory For Dynamical Systems," *Proc. 24th Conf. on Decision and Control*, Fort Lauderdale, Fla., Dec. 11-13, 1985.

Arimoto, S., Kawamura, S., and Miyazaki, F., 1984, "Bettering Operation of Robots by Learning," *Journal of Robotic Systems*, Vol. 1, No. 2, 1984, pp. 123-140.

Atkeson, C. G., and McIntyre, J., 1986, "Robot Trajectory Learning Through Practice," *Proceedings of the 1986 IEEE International Conference on Robotics and Automation*, San Francisco, Apr. 1986.

Bayard, D. S., and Wen, J. T., 1988, "New Class of Control Laws for Robotic Manipulators — Part 2. Adaptive Case," *International Journal of Control*, Vol. 47, No. 5, 1988, pp. 1387-1406.

Craig, J. J., Hsu, P., and Sastry, S. S., 1986, "Adaptive Control of Mechanical Manipulators," *Proceedings of the 1986 IEEE International Conference on Robotics and Automation*, San Francisco, Apr. 1986 (also in *The International Journal of Robotic Research*, Vol. 6, No. 2, 1987, pp. 16-28.)

Dubowsky, S., and DesForges, D. T., 1979, "The Application of Model-Reference Adaptive Control to Robotic Manipulators," *ASME JOURNAL OF DYNAMIC SYSTEMS, MEASUREMENT, AND CONTROL*, Vol. 101, pp. 193-200.

Hara, S., and Yamamoto, Y., 1985, "Stability of Repetitive Control Systems," *Proc. 24th Conf. on Decision and Control*, Fort Lauderdale, Fla., Dec. 11-13, 1985.

Horowitz, R., and Tomizuka, M., 1980, "An Adaptive Control Scheme for Mechanical Manipulators—Compensation of Nonlinearity and Decoupling Control, ASME Paper #80-WA/DSC-6 (also in *ASME JOURNAL OF DYNAMIC SYSTEMS, MEASUREMENT, AND CONTROL*, Vol. 128, No. 2, June 1986, pp. 127-135).

Horowitz, R., Kao, W. W., and Boals, M., 1989, "Digital Implementation of Repetitive Controllers for Robotic Manipulators," *Proc. of 1989 IEEE Int. Conference on Robotics and Automation*, Vol. 3, pp. 1497-1503.

Kang, C. G., Kao, W. W., Boals, M., and Horowitz, R., 1988, "Modeling Identification and Simulation of a Two Link SCARA Manipulator," in *Symposium on Robotics*, edit. K. Youcef-Toumi and H. Kazerooni, ASME 1988 Winter Annual Meeting, pp. 393-407.

Kholsa, P., and Kanade, T., 1985, "Parameter Identification of Robot Dynamics," *Proc. 24th Conf. on Decision and Control*, Fort Lauderdale, Fla., 1985, pp. 1754-1760.

Kodistchek, D. E., 1984, "Natural Motion for Robot Arms," *Proc. 23rd Conf. on Decision and Control*, Las Vegas, Nevada, Dec. 1984.

Narendra, K. S., and Valavani, L. S., 1980, "A Comparison of Lyapunov and Hyperstability Approaches to Adaptive Control of Continuous Systems," *IEEE Trans. on Automatic Control*, Vol. AC-25, No. 2, pp. 243-240.

Sadegh, N., 1987, "Adaptive Control of Mechanical Manipulators: Stability and Robustness Analysis," Ph.D. dissertation, University of California at Berkeley, Sept. 1987.

Sadegh, N., and Horowitz, R., 1987a, "Stability Analysis of an Adaptive Controller for Robotic Manipulators," *Proc. of 1987 IEEE Int. Conference on Robotics and Automation*, Vol. 3, pp. 1223-1229.

Sadegh, N., and Horowitz, R., 1987b, "Stability and Robustness Analysis of a Class of Adaptive Controllers for Robotic Manipulators," *Robotics and Automation, and Manufacturing Program, Engineering Systems Research Center, Paper No. RAMP 87-1/ESRC 87-6*, University of California at Berkeley (also to appear in *The International Journal of Robotics Research*, June 1990).

Slotine, J., and Li, W., 1986, "On the Adaptive Control of Robot Manipulators, in *Robots: Theory and Applications*," ed. by Paul, F. and Youcef-Toumi, K., *Proc. of ASME, Winter Annual Meeting, 1986* (also in *The International Journal of Robotic Research*, Vol. 6, No. 3, 1987, pp. 49-59).

Takegaki, M., and Arimoto, S., 1981, "An Adaptive Trajectory Control of Manipulators," *International Journal of Control*, Vol. 34, pp. 219-230.

Tsai, M. C., Anwar, G., and Tomizuka, M., 1988, "Discrete Time Repetitive Control for Robot Manipulators," *Proceedings of the 1988 IEEE Int. Conference on Robotics and Automation*, Apr. 1988, pp. 1341-1346.

Wen, J. T., and Bayard, D. S., 1988, "New Class of Control Laws for Robotic Manipulators — Part I. Non-adaptive Case," *International Journal of Control*, Vol. 47, No. 5, 1988, pp. 1361-1385.

APPENDIX

(A.1) Lemma: Let $f: [t_1, t_2] \rightarrow \mathbf{R}^+$ be differentiable and its derivative be upper bounded by $k^2 = \sup_{t \in [t_1, t_2]} \dot{f}(t)$ and $\epsilon > 0$, and assume that for any $s_1, s_2 \in [t_1, t_2]$ and $0 < s_2 - s_1 \leq \Delta t$, we have $\int_{s_1}^{s_2} f dt \leq \epsilon^2 \Delta t$.

Then: $f(t_2) - f(t_1) \leq \epsilon^2 + \sqrt{2\Delta t k \epsilon}$.

Proof

Let t^* be such that $f(t^*)$ is the maximum of $f(t)$ on $[t_1, t_2]$. Define $\delta^* = \sqrt{2\Delta t \frac{\epsilon}{k}}$. We now consider the following two cases:

Case (i): $t^* - t_1 < \delta^*$

For this case,

$$f(t^*) - f(t_1) = \int_{t_1}^{t^*} \dot{f}(\tau) d\tau \leq k^2(t^* - t_1) \leq \sqrt{2\Delta t k \epsilon}.$$

Since $f(t_2) \leq f(t^*)$, we have

$$f(t_2) - f(t_1) \leq \sqrt{2\Delta t k \epsilon}.$$

Case (ii): $t^* - t_1 \geq \delta^*$

Notice that

$$f(t^*) - f(\tau) = \int_{\tau}^{t^*} \dot{f}(s) ds \leq k^2(t^* - \tau).$$

Hence, for $\delta \leq \min(\Delta t, t^* - t_1)$, we obtain

$$\int_{t_1}^{t^*} f(t^*) d\tau \leq \int_{t_1}^{t^*} f(\tau) d\tau + \int_{t_1}^{t^*} k^2(t^* - \tau) d\tau$$

$$\delta f(t^*) \leq \epsilon^2 \Delta t + \frac{k^2 \delta^2}{2}. \quad (\text{A.1})$$

Dividing both sides of (A.1) by δ , we obtain

$$f(t^*) \leq \frac{\epsilon^2 \Delta t}{\delta} + \frac{1}{2} k^2 \delta. \quad (\text{A.2})$$

Let $\delta_m = \min(\Delta t, \delta^*)$. Since $t^* - t_1 \geq \delta^*$, clearly $\delta_m \leq \min(\Delta t, t^* - t_1)$, and

$$f(t^*) \leq \frac{\epsilon^2 \Delta t}{\delta_m} + \frac{k^2 \delta m}{2} \quad (\text{A.3})$$

Notice that we have defined δ^* to be the value that sets the derivative of the right-hand side of (A.3) with respect to δ_m to be zero. Hence if:

$$(a) \delta_m = \delta^*:$$

For this case, the minimum occurs at δ^* so that

$$f(t^*) \leq \sqrt{2\Delta t} k\epsilon \quad (\text{A.4})$$

$$(b) \delta_m = \Delta t,$$

$$f(t^*) \leq \epsilon^2 + \sqrt{\frac{\Delta t}{2}} k\epsilon \quad (\text{A.5})$$

Combining (A.4) and (A.5),

$$f(t^*) \leq \epsilon^2 + \sqrt{2\Delta t} k\epsilon$$

Since $f(t_1), f(t_2) \leq f(t^*)$, we have

$$f(t_2) - f(t_1) \leq \epsilon^2 + \sqrt{\frac{\Delta t}{2}} k\epsilon$$

Proof of Lemma (6.2)

Part (i)

From equations (6.11) and (6.12), we obtain:

$$\begin{aligned} \Delta V(j, k) &= \frac{1}{2} \int_{t_{jk}}^{t_{j(k+1)}} \frac{d}{dt} \left\{ \bar{\mathbf{e}}^T(t) \bar{\mathbf{e}}(t) \right\} dt \\ &+ \frac{1}{2} \tilde{\mathbf{w}}_d^T(j+1, k) \mathbf{K}_L^{-1} \tilde{\mathbf{w}}_d(j+1, k) - \frac{1}{2} \tilde{\mathbf{w}}_d^T(j, k) \mathbf{K}_L^{-1} \tilde{\mathbf{w}}_d(j, k) \end{aligned} \quad (\text{A.6})$$

Utilizing the expression for the error dynamics in equation (5.7) and the results in equation (5.11), we obtain

$$\begin{aligned} \Delta V(j, k) &\leq \int_{t_{jk}}^{t_{j(k+1)}} \left\{ -\mathbf{e}_v^T(t) \mathbf{F}_{v1} \mathbf{e}_v(t) \right. \\ &\quad \left. - \bar{\lambda}_p \mathbf{e}^T(t) \mathbf{F}_p \mathbf{e}(t) + \mathbf{e}_v^T(t) \tilde{\mathbf{w}}_r(t) \right\} dt \\ &+ \frac{1}{2} \tilde{\mathbf{w}}_d^T(j+1, k) \mathbf{K}_L^{-1} \tilde{\mathbf{w}}_d(j+1, k) - \frac{1}{2} \tilde{\mathbf{w}}_d^T(j, k) \mathbf{K}_L^{-1} \tilde{\mathbf{w}}_d(j, k) \end{aligned} \quad (\text{A.7})$$

From equations (6.8)–(6.10)

$$\begin{aligned} \Delta V(j, k) &\leq \int_{t_{jk}}^{t_{j(k+1)}} \left\{ -\mathbf{e}_v^T(t) \mathbf{F}_{v1} \mathbf{e}_v(t) \right. \\ &\quad \left. - \bar{\lambda}_p \mathbf{e}^T(t) \mathbf{F}_p \mathbf{e}(t) + \mathbf{e}_v^T \Delta \mathbf{w}_d(t) \right\} dt \\ &+ \frac{1}{2} \tilde{\mathbf{w}}_d^T(j+1, k) \mathbf{K}_L^{-1} \tilde{\mathbf{w}}_d(j+1, k) - \frac{1}{2} \tilde{\mathbf{w}}_d^T(j, k) \mathbf{K}_L^{-1} \tilde{\mathbf{w}}_d(j, k) \\ &\quad + \tilde{\mathbf{w}}_d^T(j, k) \int_{t_{jk}}^{t_{j(k+1)}} \mathbf{e}_v(t) dt \end{aligned} \quad (\text{A.8})$$

Utilizing the “learning” control law in equations (6.4)–(6.6), we obtain

$$\frac{1}{2} \tilde{\mathbf{w}}_d^T(j+1, k) \mathbf{K}_L^{-1} \tilde{\mathbf{w}}_d(j+1, k)$$

$$\begin{aligned} -\frac{1}{2} \tilde{\mathbf{w}}_d^T(j, k) \mathbf{K}_L^{-1} \tilde{\mathbf{w}}_d(j, k) &= \frac{1}{2} \mathbf{e}_v^{*T}(j, k) \mathbf{K}_L \mathbf{e}_v^*(j, k) \\ &- \tilde{\mathbf{w}}_d^T(j, k) \mathbf{e}_v^*(j, k) \end{aligned} \quad (\text{A.9})$$

Thus,

$$\begin{aligned} \Delta V(j, k) &\leq \int_{t_{jk}}^{t_{j(k+1)}} \left\{ -\mathbf{e}_v^T(t) \mathbf{F}_{v1} \mathbf{e}_v(t) \right. \\ &\quad \left. - \bar{\lambda}_p \mathbf{e}^T(t) \mathbf{F}_p \mathbf{e}(t) + \mathbf{e}_v^T \Delta \mathbf{w}_d(t) \right\} dt \\ &+ \frac{1}{2} \mathbf{e}_v^{*T}(j, k) \mathbf{K}_L \mathbf{e}_v^*(j, k) \end{aligned} \quad (\text{A.10})$$

By the Schwartz's inequality

$$|\mathbf{e}_v^*(j, k)| \leq \Delta t^2 \left[\int_{t_{jk}}^{t_{j(k+1)}} |\mathbf{e}_v(t)|^2 dt \right]^{\frac{1}{2}} \quad (\text{A.11})$$

From equations (A.10) and (A.11),

$$\begin{aligned} \Delta V(j, k) &\leq \int_{t_{jk}}^{t_{j(k+1)}} \left\{ -\mathbf{e}_v^T(t) \left[\mathbf{F}_{v1} - \frac{1}{2} \Delta t \mathbf{K}_L \right] \mathbf{e}_v(t) \right. \\ &\quad \left. - \bar{\lambda}_p \mathbf{e}^T(t) \mathbf{F}_p \mathbf{e}(t) + \mathbf{e}_v^T \Delta \mathbf{w}_d(t) \right\} dt \end{aligned} \quad (\text{A.12})$$

Adding and subtracting the term

$$\int_{t_{jk}}^{t_{j(k+1)}} \left\{ \frac{h^2}{4} |\Delta \mathbf{w}_d(t)|^2 + \frac{1}{h^2} |\mathbf{e}_v|^2 \right\} dt$$

in equation (A.12), we obtain

$$\begin{aligned} \Delta V(j, k) &\leq \int_{t_{jk}}^{t_{j(k+1)}} \left\{ -\mathbf{e}_v^T(t) \left[\mathbf{F}_{v1} - \frac{1}{2} \Delta t \mathbf{K}_L - \frac{1}{h^2} \mathbf{I} \right] \mathbf{e}_v(t) \right. \\ &\quad \left. - \bar{\lambda}_p \mathbf{e}^T(t) \mathbf{F}_p \mathbf{e}(t) \right\} dt \\ &- \int_{t_{jk}}^{t_{j(k+1)}} \left\{ \frac{1}{h} \mathbf{e}_v^T(t) - \frac{h}{2} \Delta \mathbf{w}_d(t) \right\}^2 dt - \frac{h^2}{4} |\Delta \mathbf{w}_d(t)|^2 dt \end{aligned} \quad (\text{A.13})$$

where the scalar h is selected such that $\left[\mathbf{F}_{v1} - \frac{1}{2} \Delta t \mathbf{K}_L - \frac{1}{h^2} \mathbf{I} \right] > \mathbf{O}$

By equation (6.10), we have:

$$\frac{h^2}{4} \int_{t_{jk}}^{t_{j(k+1)}} |\Delta \mathbf{w}_d(t)|^2 dt \leq \frac{\Delta t h^2 \overline{\Delta \mathbf{w}_d^2}}{4} \quad (\text{A.14})$$

Utilizing equations (A.13), (A.14) and (6.6), we obtain

$$\Delta V(j, k) \leq \left[-\lambda_v + \frac{1}{h^2} \right] \left\{ \bar{\epsilon}^{*2} - \left[\frac{h^4}{h^2 \lambda_v - 1} \right] \frac{\Delta t \overline{\Delta \mathbf{w}_d^2}}{4} \right\} \quad (\text{A.15})$$

The second term in equation (A.15) is minimized with respect to h by selecting $h^2 = 2/\lambda_v$. Thus, by choosing:

$$\kappa_p = \frac{\bar{\lambda}_p}{\lambda_v} \quad (\text{A.16})$$

and

$$\epsilon^2 \geq \left[\frac{\overline{\Delta \mathbf{w}_d}}{\lambda_v} \right]^2 \quad (\text{A.17})$$

we get:

$$\Delta V(j, k) \leq -\frac{\lambda_v}{2} (\bar{\epsilon}^{*2} - \epsilon^2 \Delta t) \quad (\text{A.18})$$

Part (ii)

We now consider the time intervals in which the learning is frozen. First, note that the signal $\tilde{\mathbf{w}}_d$ remains bounded by the virtue of the projection algorithm, equation (5.6). In fact, from (5.3b) we have: $|\tilde{\mathbf{w}}_d(t_{jk})|^2 \leq r_w^2$ for all t_{jk} 's. Let us define the following Lyapunov function:

$$\mathbf{V}_1 = \frac{1}{2} \bar{\mathbf{e}}^T(t_{jk}) \bar{\mathbf{e}}(t_{jk}). \quad (\text{A.19})$$

Similarly to the proof of part (i), the derivative of \mathbf{V}_1 can be estimated as follows:

$$\frac{d}{dt} \mathbf{V}_1 \leq \frac{\overline{\Delta \mathbf{w}_d^2} + \bar{\mathbf{w}}_d^2}{\lambda_v} \leq \epsilon^2 \lambda_v + \frac{r_w^2}{\lambda_v} = k^2. \quad (\text{A.20})$$

The next step is to estimate $\int_{t_{jk}}^{t_{j(k+1)}} \mathbf{V}_1(\tau) d\tau$. By some algebra,

from equations (A.17) and (6.13)–(6.16), $\mathbf{V}_1 \leq \frac{1}{2} \lambda_v \rho e^{*2}$. Thus

$$\int_{t_{jk}}^{t_{j(k+1)}} \mathbf{V}_1(\tau) d\tau \leq \frac{1}{2} \lambda_v \rho \epsilon^2 \Delta t.$$

Now, consider $s_1, s_2 \in [t_{jk}, t_{jm}]$. Consider the following cases:

Case (i): $m = k + 1$

In this case,

$$\int_{s_1}^{s_2} \mathbf{V}_1(\tau) d\tau \leq \int_{t_{jk}}^{t_{j(k+1)}} \mathbf{V}_1(\tau) d\tau \leq \frac{1}{2} \lambda_v \rho \epsilon^2 \Delta t$$

Case (ii): $m \geq k + 2$

In this case, let $t_{jk} \leq t_i \leq s_1 < t_{i+1} \leq s_2 \leq t_{jm}$, then

$$\int_{s_1}^{s_2} \mathbf{V}_1(\tau) d\tau \leq \int_{t_i}^{t_{i+1}} \mathbf{V}_1(\tau) d\tau + \int_{t_{i+1}}^{t_{i+2}} \mathbf{V}_1(\tau) d\tau \leq \lambda_v \rho \epsilon^2 \Delta t$$

Invoking the result of lemma (A.1), we conclude that $\mathbf{V}_1(t_{jm}) - \mathbf{V}_1(t_{jk}) \leq \alpha_2 \epsilon^2 + \alpha_2 \epsilon$ for all t 's in which the learning is frozen, where

$$\begin{aligned} \alpha_1 &= (\rho + \sqrt{2\rho\Delta t}) \lambda_v \\ \alpha_2 &= \sqrt{2\rho\Delta t} r_w \end{aligned} \quad (\text{A.21})$$